

**Twilight observations from a balloon gondola
Preliminary results**

by M. ACKERMAN, C. LIPPENS and C. MULLER

Belgian Institute for Space Aeronomy
Circular Avenue 3, B - 1180 Brussels

and by P. VRIGNAULT (*)

Centre d'Essais des Landes, F - 40520 Biscarosse

Abstract. — Twilight data obtained photographically from a stratospheric balloon platform in the falls of 1980 and 1981 and in the spring of 1982 are presented for blue and red light. They indicate the presence of a dust light absorbing and scattering layer in the mesosphere at altitudes near 60 km with a low scattering albedo (0.1) at 0.44 μm . The optical efficiency of the layer increases more than 10 times when the wavelength of the interacting light changes from 0.65 μm to 0.44 μm . At the zenith and near sunset, the natural 0.44 μm extinction optical thickness and the cm^2 column scattering rate due to this layer are respectively found to be 6.6×10^{-2} and 0.18 mega Rayleigh per Å on May 3, 1982 above the south west of France.

The observations are presented in the framework of other data derived from ground, aircraft, balloons and spacecraft observations.

1. INTRODUCTION

A long time before the space age started the observation of the twilight has been an important source of information about the upper atmosphere. Even recently stratospheric trace species such as NO_2 have been studied through sky observations at large solar zenith angles.

One of the most thorough investigations of this kind has been reported by Volz and Goody [1] who pointed out the resources and

(*) Présentés par M. M. NICOLET.

drawbacks of such a work. One of their conclusions indicates well the complexity of the phenomena involved: "when we understand the twilight of the earth to the extent that all its features can be explained numerically, we will be in a position to analyze fly-by observations on Mars and Venus". We know presently that this is an understatement.

When twilight observation takes place from the ground aiming at the determination of upper atmospheric properties, the variability of the optical properties of the troposphere, the vicinity of city lights and other factors add complexity to the understanding of the measured sky radiance generally expressed in terms of solar radiance. The observation of these quantities from high altitude platforms leads to a more simple interpretation and gives access to parameters unattainable from the ground. Much of the twilight work has been devoted to the search for dust in the atmosphere in order to determine its possible role in the radiation balance of the earth and in photochemical atmospheric processes.

Aerosols have already been optically observed in the upper atmosphere from spacecrafts [2-3] and rockets [4-6]. Twilight observations [1-7] are also consistent with an upper atmospheric particulate scattering. Other relevant experimental and theoretical work about upper atmospheric aerosols has been reviewed recently [8] in a study of their possible continuous and sporadic extraterrestrial sources and fate. On the other hand it has been known for more than forty years [9] that the atmosphere contains an other source of optical extinction than air and ozone in a supposedly most transparent spectral region around $0,44 \mu\text{m}$. This extinction has been observed day and night using stars and the sun as light sources and has caused some concern to various authors [10-12] interested in the accurate determination of the extraterrestrial solar flux. These authors have attributed the extra-extinction to aerosols. It has more recently been attributed entirely to NO_2 [13-14] but the amount of this atmospheric constituent so deduced is in disagreement with observations based on the NO_2 extinction of infrared radiation [15-17] and based on the differential extinction measurement of blue night [18-23]. Both last methods yield a smaller nitrogen dioxide abundance, ten to hundred times less. Several authors [20-21, 23] have indicated the presence of an unattributed absorption at $0,44 \mu\text{m}$ in the upper stratosphere.

2. OBSERVATION METHOD

The observation method used here has been described previously [24] and leads to the determination for various scattering angles, θ , of the radiance of the sunlit atmosphere in units of solar radiance is given by

$$R_{\theta}/R_{\odot} = 6.79 \times 10^{-5} [(Q_s n \sigma \varphi_{\theta}/4\pi) + n_M \sigma_{\theta}] \quad (1)$$

Where Q_s , σ , φ_{θ} and n are the aerosol scattering efficiency, the geometrical cross section, the phase function and the number of particles on the line of sight and where n_M and σ_{θ} are the number of air molecules on the line of sight and the differential air scattering cross section [25].

Two improvements were implemented in the gondola. A neutral density filter identical to the one used to photograph the sun at elevation angles larger than 5° was remotely moved in front of the cameras in order to photograph the solar image at zenith angles from 76° to 95° allowing to perform atmospheric absorption measurements. When the sun was at elevation angles larger than 5° , the lower neutral density screens being removed from the cameras field of view, the gondola was rotated about its vertical axis by steps of 36° in order to obtain overlapping pictures of the earth limb. The spectral bandwidths were $0.66 \mu\text{m}$ and $0.10 \mu\text{m}$ centered at $0.44 \mu\text{m}$ and $0.65 \mu\text{m}$ respectively as shown in figure 1.

The solar irradiance, I_0 , is attenuated by the atmosphere leading to the measured irradiance

$$I = I_0 e^{-\tau} \quad (2)$$

where the optical thickness

$$\tau = \Sigma (\sigma_g n_g) + [(Q_s + Q_a) n \sigma] \quad (3)$$

where, σ_g and n_g are the extinction cross section of atmospheric gases and their numbers of molecules on the optical path whereas Q_a is the absorption efficiency of the aerosol. Q_s , n and σ have been defined in (1). The scattering albedo of the aerosol is

$$\omega = \frac{Q_s}{Q_s + Q_a} \quad (3)$$

and the extinction efficiency of the aerosol is

$$Q_e = Q_s + Q_a \quad (5)$$

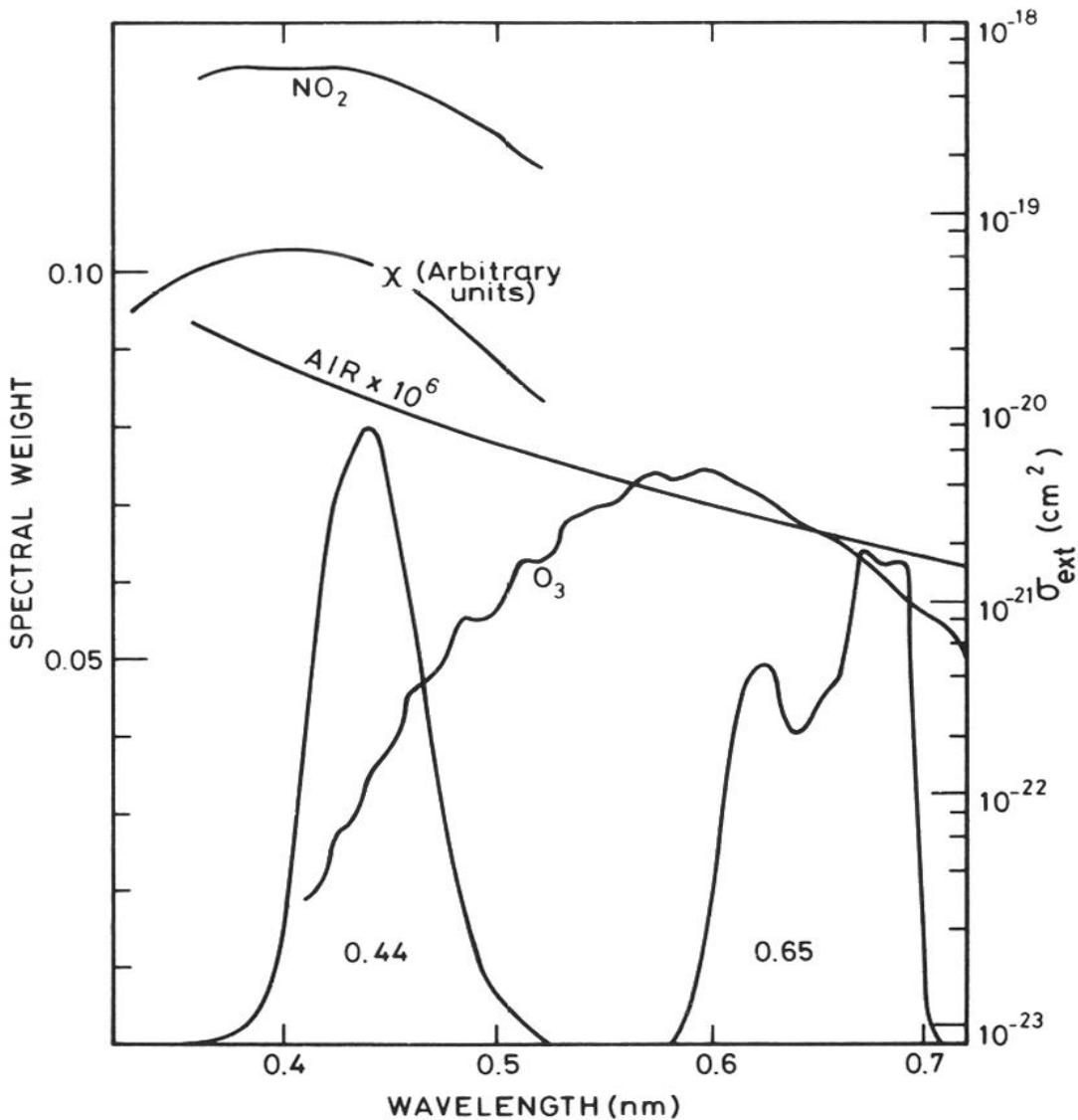


FIG. 1. — Spectral weight of the filters and solar radiation combination showing the spectral bandpass response of the cameras at 0.44 and at 0.65 μm . The extinction cross sections for air, ozone and nitrogen dioxide are also shown. The spectral distribution (13) of the excess extinction is also shown.

3. THE OBSERVATIONS

a. *Sunlight Extinction*

The balloon flight took place from Aire sur l'Adour in the afternoon of October 19, 1981. During the ascent in the stratosphere and at ceiling altitude, the winds carried the balloon mainly southward in

such a way that observations took place near 43 °N and 0°30' West from 15.30 to 17.30 hrs GMT. Radar tracking was performed by the Centre d'Essais des Landes using a transponder carried with the gondola. Temperature and wind and ozone soundings were made, respectively starting at 10.59 and 13.36 hrs G.M.T. from 44°21'N and 1°14'W. From the beginning of the scattering measurements to the end of the absorption measurements the balloon altitude decreased from 34.3 to 33.2 km.

The observed solar irradiances, I , at 0.44 μm are plotted versus solar zenith angles, χ° , in figure 2 as well as their theoretically evaluated evolutions from $\chi = 91^\circ$ towards smaller and larger values of χ . Rayleigh extinction by air has only been taken into account and

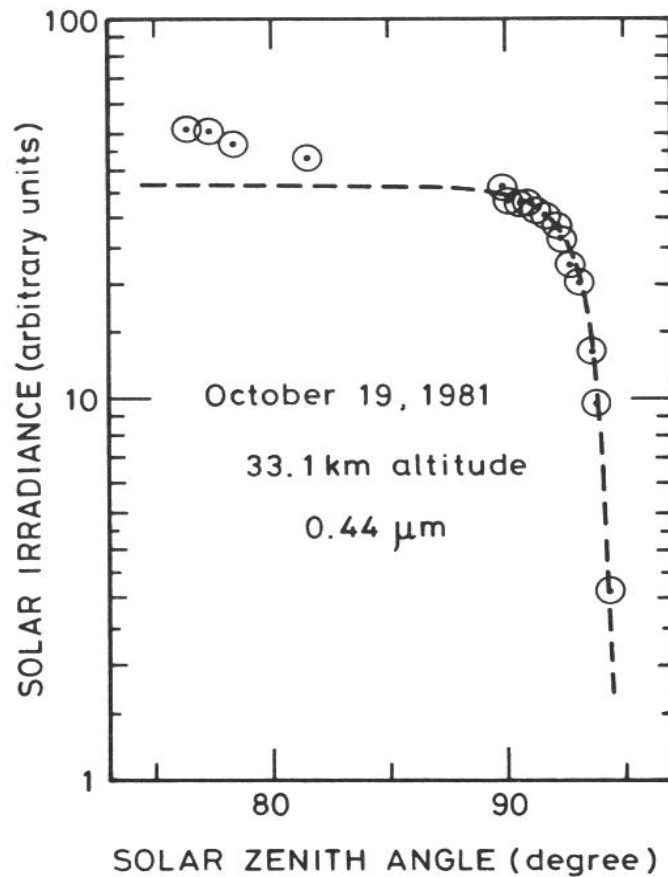


FIG. 2. — Solar irradiances in arbitrary units versus solar zenith angles in degrees observed on October 19, 1981. The circles represent the measurements while the dashed curve represents the expected variation from Rayleigh extinction, the main expected component at 0.44 μm . The observed solar irradiance at $\chi = 91^\circ$ has been taken as a baseline for the computation.

represents fairly well the change of I from $\chi = 91^\circ$ to $\chi = 94.3^\circ$. A small maximum of excess extinction is observed centered at $\chi = 92.5^\circ$. It corresponds to an optical thickness $\tau \cong 0.06$ which, if attributed to NO_2 , leads to an integrated amount on the optical path equal to 10^{17} molecules per cm^2 at 28 km grazing altitude, a small value, if compared with previous determinations.

We however wish to point out the difference between the theoretically expected and the observed evolution of I in the range $90^\circ < \chi < 76^\circ$. An excess of extinction decreasing slowly with increasing solar elevation is observed. This excess has been reported previously by several authors as shown in table I. Its slow evolution with zenith angle indicates that its cause lies well above flight altitude. No presently known gaseous absorber can explain the observed extinction. At $0.65 \mu\text{m}$, an optical thickness change equal to 0.1 can be detected in the measurements from $\chi = 76^\circ$ to $\chi = 90^\circ$ corresponding within experimental uncertainties to the expected variation of the ozone extinction. This leads to the first conclusion that a spectrally selective extinction takes place in the upper atmosphere at $0.44 \mu\text{m}$, of which the origin is up to now unknown. Assuming that the Chapman function is valid for $\chi < 75^\circ$, the total optical thickness at $0.44 \mu\text{m}$ on

TABLE 1. — List of extinctions in excess of Rayleigh scattering extinction observed at or near $0.44 \mu\text{m}$ and at solar zenith angles $\chi \cong 90^\circ$ by means of instruments flown on various dates at various altitudes in the stratosphere. The changes of optical thickness, $\Delta\tau$, are indicated for various ranges of zenith angles. The observations made from Concorde in June-July 1973 lead to an absolute value of τ deduced from absolute solar irradiance data measured at 16 km altitude and $\chi = 90^\circ$ compared with extraterrestrial solar flux values.

Date	Flight altitude (km)	Range of χ	Wavelength (nm)	$\Delta\tau$	Reference
Feb. 9, 1977	40	75-80	445	0.18	(20)
Oct. 15, 1980	38	81-84	440	0.28	This work [24]
Oct. 19, 1981	34.1	76-82	440	0.19	This work
Id.	34.1	82-90	440	0.22	This work
June-July 1973	16.0	$90^\circ \rightarrow \odot$	430	0.57	(13)

(*) τ has been deduced from a least square fit to the data available in this range of χ° .

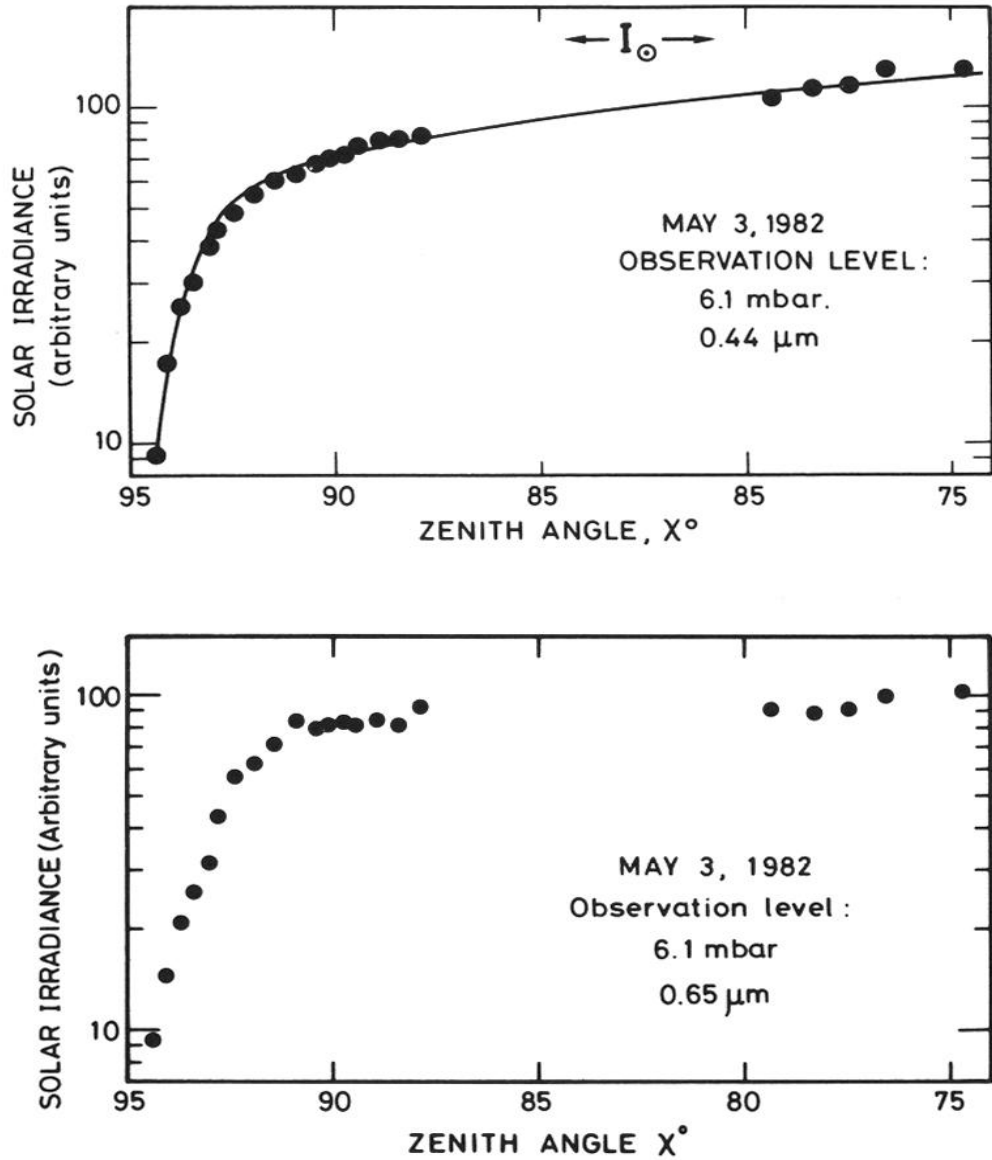


FIG. 3. — a) Solar irradiance observed on May 3, 1982 from a flight level of 6.1 mbar at 0.44 μm versus solar zenith angles χ . The values represented by the solid curve have been computed taking the extinction optical thicknesses shown in figure 4 and the extraterrestrial solar irradiance indicated by the arrows (I_\odot).

b) Same as a) but for 0.65 μm . The only absorber which can be considered in this case at $\chi = 90$ is O_3 leading in this case to a radiance reduction equal to 12%. No excess extinction can be detected in this case with certainty.

October 19, 1981 at $\chi = 90^\circ$ and at 34 km altitude may approach unity.

On May 3, 1982, an other evening flight took place from Aire sur l'Adour. The gondola reached a ceiling pressure level equal to 6.1 mb with a maximum radar measured altitude equal to 36.6 km. The solar extinction data are shown in figure 3a. Here again an excess extinction appears at $0.44 \mu\text{m}$ for solar zenith angles smaller than 90° . Figure 3b shows the solar extinction curve at $0.65 \mu\text{m}$. Taking into account an optical thickness equal to 0.1 in red light due to ozone at a zenith angle of 90° , no additional or excess absorption can be measured.

The solid curve fitting the data on figure 3a is the result of a computation taking into account the optical thickness variation versus zenith angle shown in figure 4 for air (Rayleigh scattering), NO_2 and X, the unknown absorber.

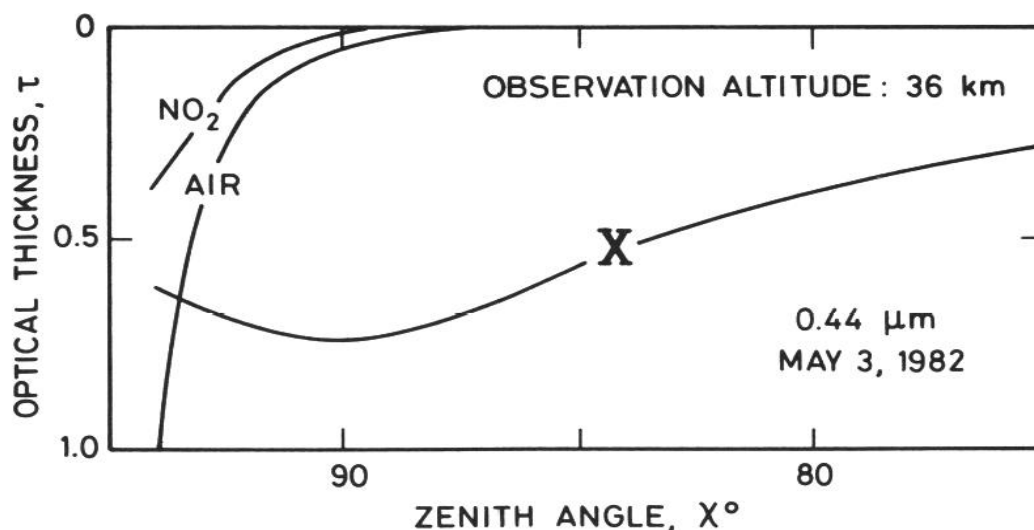


FIG. 4. — Optical extinction thicknesses due to air, NO_2 and to the excess absorber, X, necessary to interpret the extinction observations of figure 3a.

In order to evaluate the effective altitude of X, the fraction of the maximum optical thickness τ , reached at $\chi = 90^\circ$, has been computed for various values of χ . The result is shown in figure 5. The relative value of the extraterrestrial solar radiance indicated in the figure has been chosen to provide the best fit to a theoretical dependence of τ versus χ leading to an effective altitude equal to 60 ± 10 km.

The NO_2 optical thickness shown in figure 4 associated with a molecular extinction cross section equal to $6 \times 10^{-19} \text{ cm}^2$ leads to the

vertical nitrogen dioxide distribution shown in figure 6. It corresponds to a total vertical content of NO_2 equal to 10^{16} molecules per cm^2 .

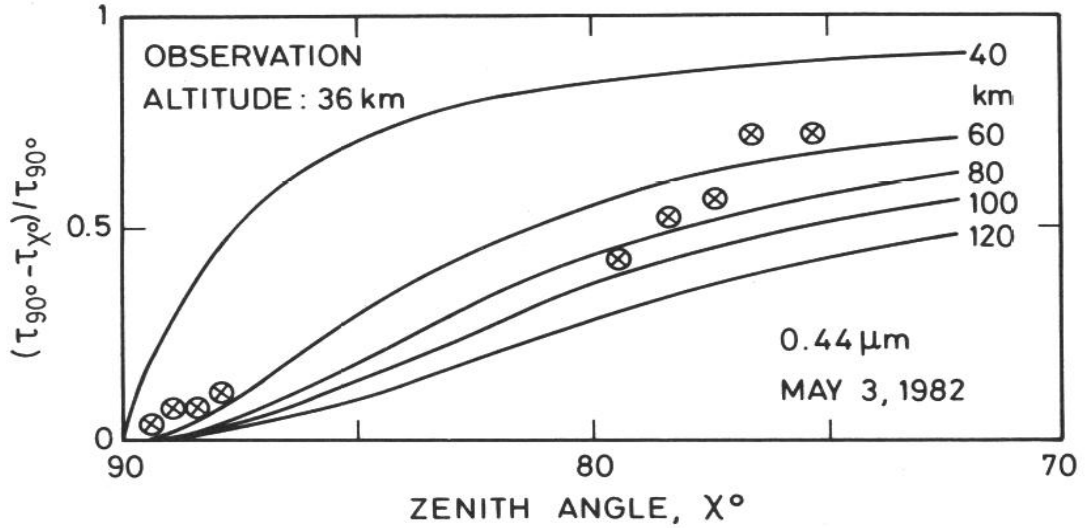


FIG. 5. — Fraction of the excess extinction at $\chi = 90$ versus zenith angles, χ . The computed variation of this quantity versus χ for various effective altitudes (40, 60, 80, 100 and 140 km) of the X absorber.

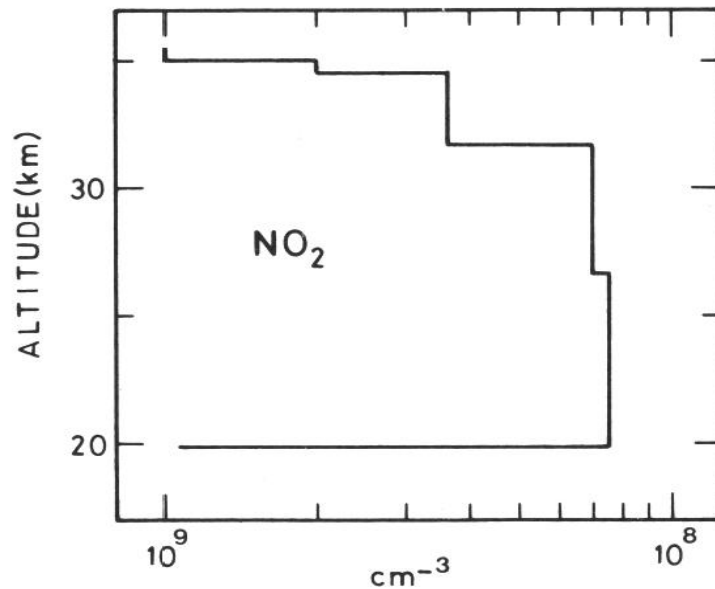


FIG. 6. — Nitrogen dioxide vertical distribution deduced from the NO_2 optical thickness shown in figure 4.

b. Atmospheric radiances

The earth limb radiances observed in the range of zenith angles, χ° , from 86° to 93° are shown in figure 7 for two flights : October 15, 1981 at 37 km altitude (only mainly forward scattering is shown at $0.44 \mu\text{m}$ and at $0.65 \mu\text{m}$) and October 19, 1981 at 34 km altitude (scattering angles from 14.5° to 166° at $0.44 \mu\text{m}$ and from 10.5° to 51° at $0.65 \mu\text{m}$). The accuracy of the absolute values of R_θ/R_\odot are considered to be $\pm 50\%$ from one camera to the next one, mostly due to the uncertainty in the evaluation of the high extinction of the neutral density screens. The accuracy of the relative values on a single camera is $\pm 5\%$. The radiance variation observed versus χ° on October 15, 1980 and shown here for $\theta = 13^\circ$ illustrates best the phenomenon that

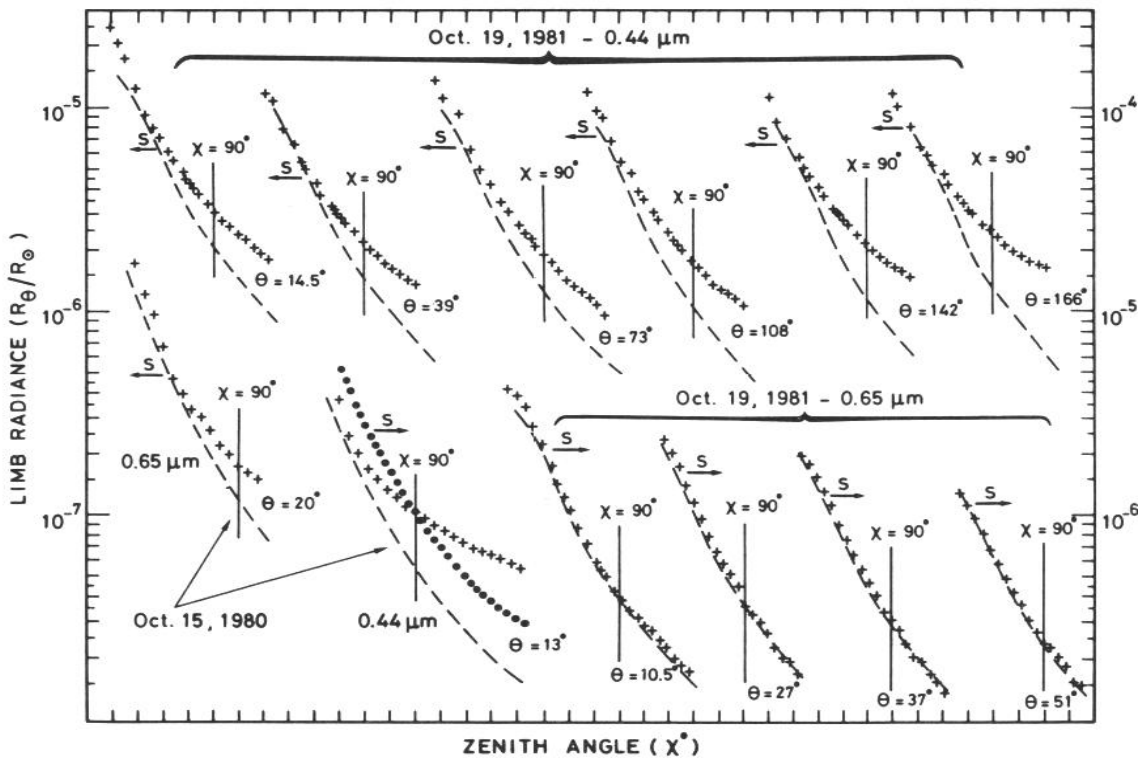


FIG. 7. — Earth limb radiance R_θ/R_\odot in units of solar radiance observed on October 15, 1980, at 37 km altitude and on October 19, 1981 at 34 km altitude versus zenith angles χ° . The observations are represented by crosses. The dashed and dotted (see text) curves represent total numbers of air molecules in arbitrary units which can be seen on the line of sight versus zenith angles χ° . The arrows marked *s* indicate the ordinate scale relevant for each graph. The scattering angles θ° , the wavelengths, $0.65 \mu\text{m}$ or $0.44 \mu\text{m}$ and the dates are also indicated. Average solar zenith angles were 78° on October 19, 1981 and 80° on October 15, 1980. For each case a vertical line indicates the $\chi = 90^\circ$ position on the abscissa where an angular difference of 1° separates two ticks.

we wish to emphasize. Since at $0.44\ \mu\text{m}$, the Rayleigh scattering should dominate the scattering, a theoretical variation, in arbitrary units, of the total number of air molecules on the line of sight versus χ is fitted to the observed radiance curve at $\chi = 90^\circ$. At χ larger and smaller than 90° the observed radiance variation with χ is smaller than the theoretical one represented by the dotted curve. The cause of this difference is considered to be an excess of radiance originating from altitudes larger than the flight altitude. The dotted theoretical curve is shifted downwards to fit the observations at $\chi \cong 92.5^\circ$ where the excess of radiance becomes small compared to the air Rayleigh radiance, since lower and lower altitudes are tangentially observed at larger and larger zenith angles where the increasing air density must eventually dominate the scattering dependence of zenith distance. It is also observed that the excess radiance decreases slowly above the horizontal line of sight when χ° becomes smaller than 90° . The same phenomenon is observed on October 19, 1981 at $0.44\ \mu\text{m}$ and at all scattering angles. In this case, however the excess appears relatively smaller since the flight altitude was lower leading to a larger Rayleigh scattering due to air. An decrease of the blue and red color ratio occurring near 1° solar depression angle, δ° , has been observed in twilight studies [1] as well as an excess of blue light at $\delta = 0^\circ$ which was attributed to multiple scattering. In the case of our observations however, the air observed at χ equal or smaller than 90° is theoretically optically thin and multiple scattering does not provide an explanation for the radiance excess, relative to pure air, linked with the anomalous radiance variation with zenith angle.

At $0.65\ \mu\text{m}$, a small excess of radiance is observed at $\theta = 20^\circ$ on October 15, 1980. It is barely detectable at $\theta = 10.5^\circ$ on October 19, 1981 and it can not be detected at larger scattering angles, being most probably too small relative to Rayleigh scattering at this low flight level.

For the May 3, 1982 flight, one of the cameras was fitted with a blue filter equipped wide angle lens ($f = 50\ \text{mm}$) instead of the lens normally used ($f = 80\ \text{mm}$). No neutral density screen was placed in front of this camera in order to view the sky over a wider range of zenith angles. The calibration of this camera was performed by comparing film optical densities of identical features simultaneously photographed by means of an other blue filter neutral density screen equipped camera.

Twilight observations from a balloon gondola

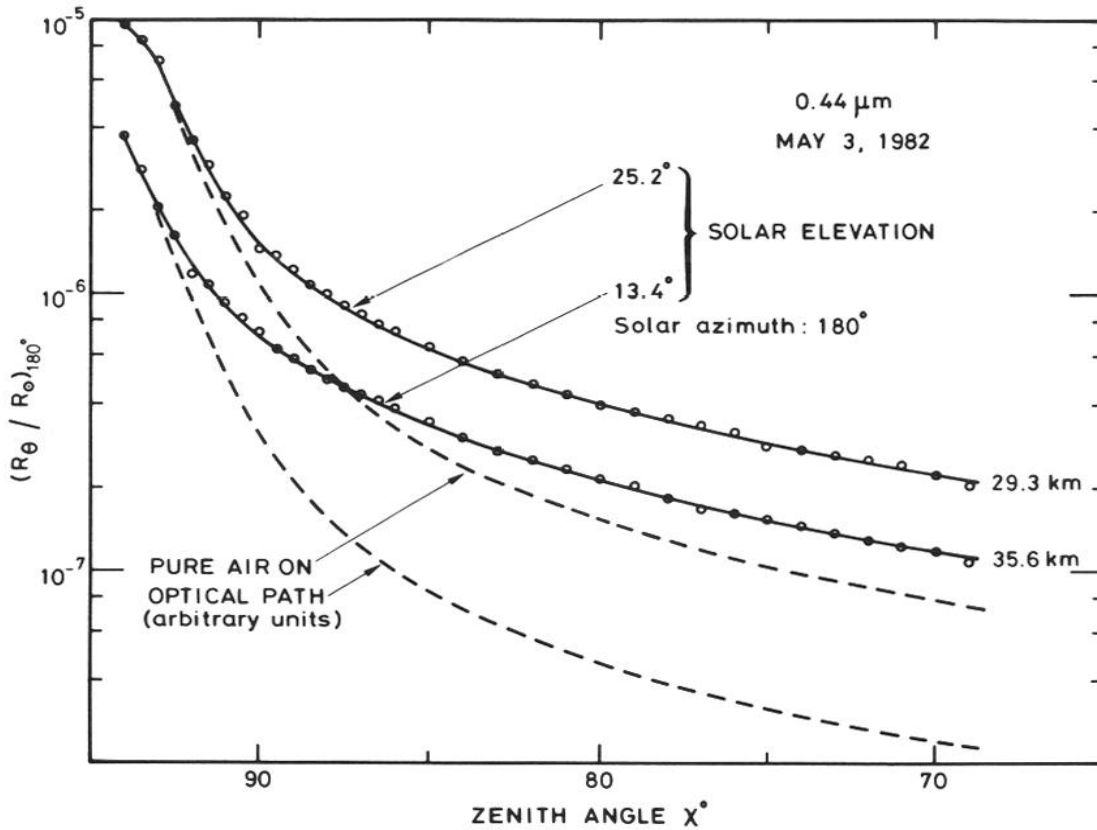


FIG. 8. — Atmospheric radiance versus zenith angle at $0.44 \mu\text{m}$ from two flight levels on May 3, 1982. As in figure 7, the pure air expected radiance is represented by the dashed curves.

The limb radiance observed at two flight levels, one during the balloon ascent and the other one at ceiling altitude are shown in figure 8 versus zenith angles. The variations of the number of air molecules viewed on the optical path versus zenith angles are also represented in arbitrary unit. They are fitted to the observations at large zenith angles (larger than 90°) where pure air Rayleigh scattering must dominate. The excess of radiance corresponding to the difference between the measured and pure air expected radiances has been determined and plotted in figure 9 versus zenith angles. The inversion observed at $\chi = 90^\circ$ clearly indicates that the excess radiance originates from altitudes higher than the flight altitude.

As for the extinction in figure 5, the fraction of the total excess radiance at $\chi = 90^\circ$ has been plotted versus zenith angles in figure 10. Here again the measurements show an effective altitude for the excess radiance near 60 km.

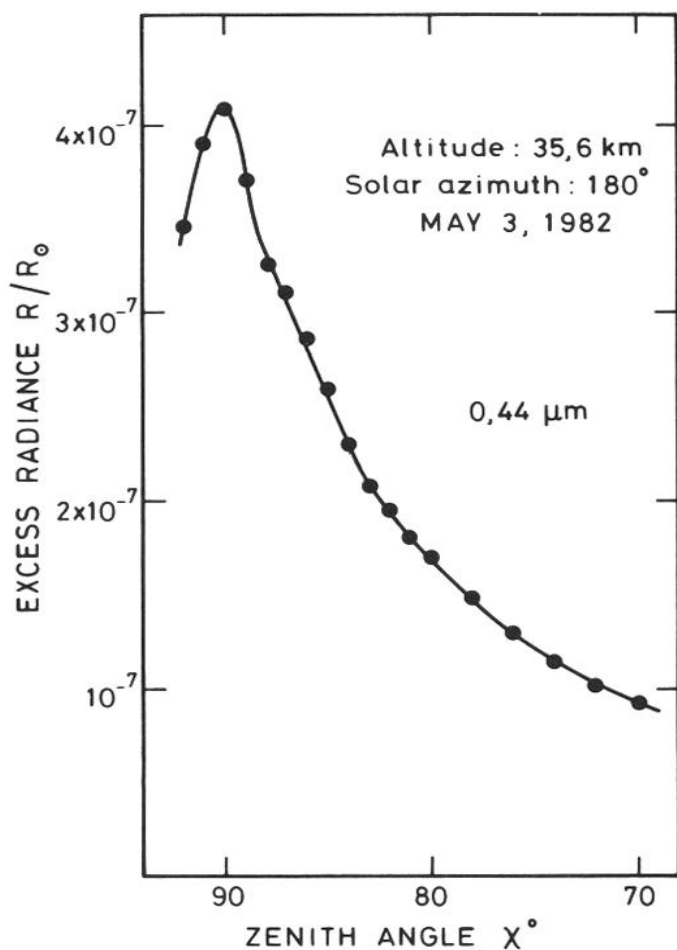


FIG. 9. — Excess radiance deduced from the 35.6 km observation data of figure 8 versus zenith angles. The inversion at $\chi = 90^\circ$ demonstrates the upper altitude origin of the excess radiance.

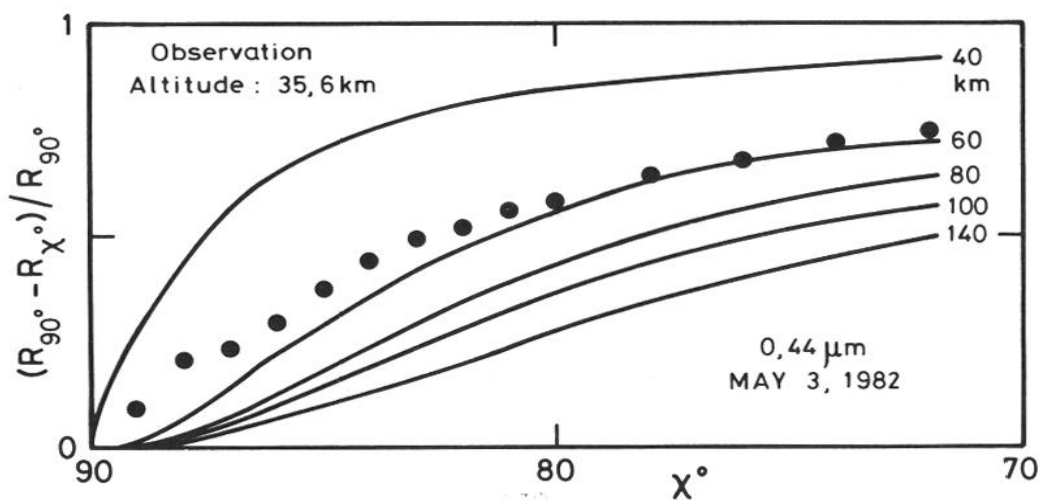


FIG. 10. — As in figure 5, the fraction of the excess radiance observed at $\chi = 90^\circ$ is shown versus χ . The expected variation of this quantity versus χ is also shown for various effective altitudes. It indicates an effective altitude of the excess radiance nearly equal to 60 km.

The radiance observed at $0.65 \mu\text{m}$ is plotted in figure 11 versus zenith angles for two flight levels as it was done in figure 8 for $0.44 \mu\text{m}$. The excess radiance determined in red light is 11 times smaller than in blue light.

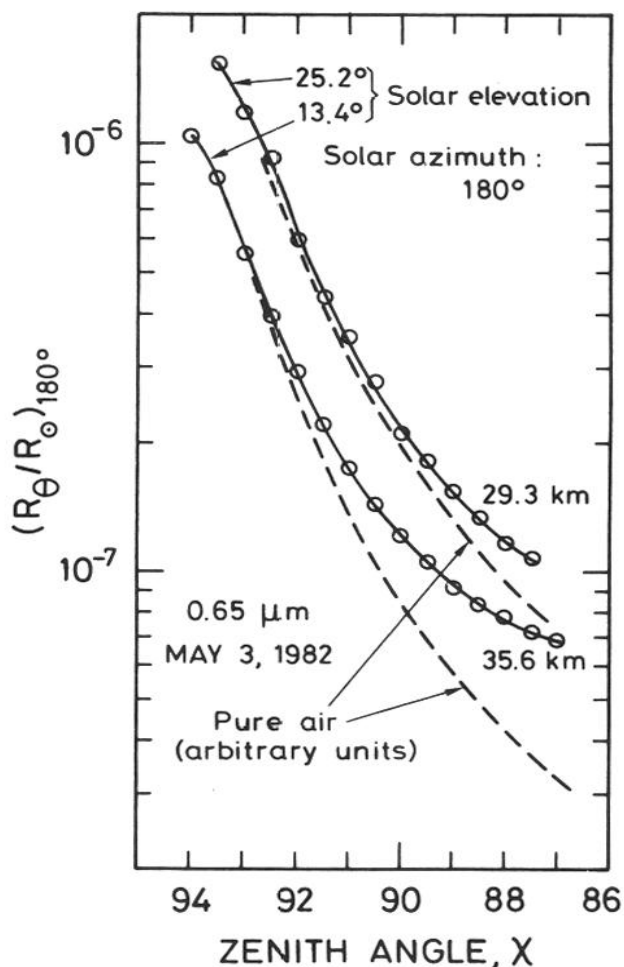


FIG. 11. — As in figure 8, the radiance observed versus zenith angles is shown, but for $0.65 \mu\text{m}$. The excess radiance observed in red light is 11 times smaller than in blue light.

By spinning the gondola about its vertical axis by steps of 36° the data necessary for the determination of the phase function of the excess radiance have been obtained and are shown for $0.44 \mu\text{m}$ in figure 12.

The phase functions are shown in figure 13 for three zenith angles in the case of the excess radiance. The values for air are those measured on figure 12 at $\chi = 90^{\circ}$. However the angular variation reflects

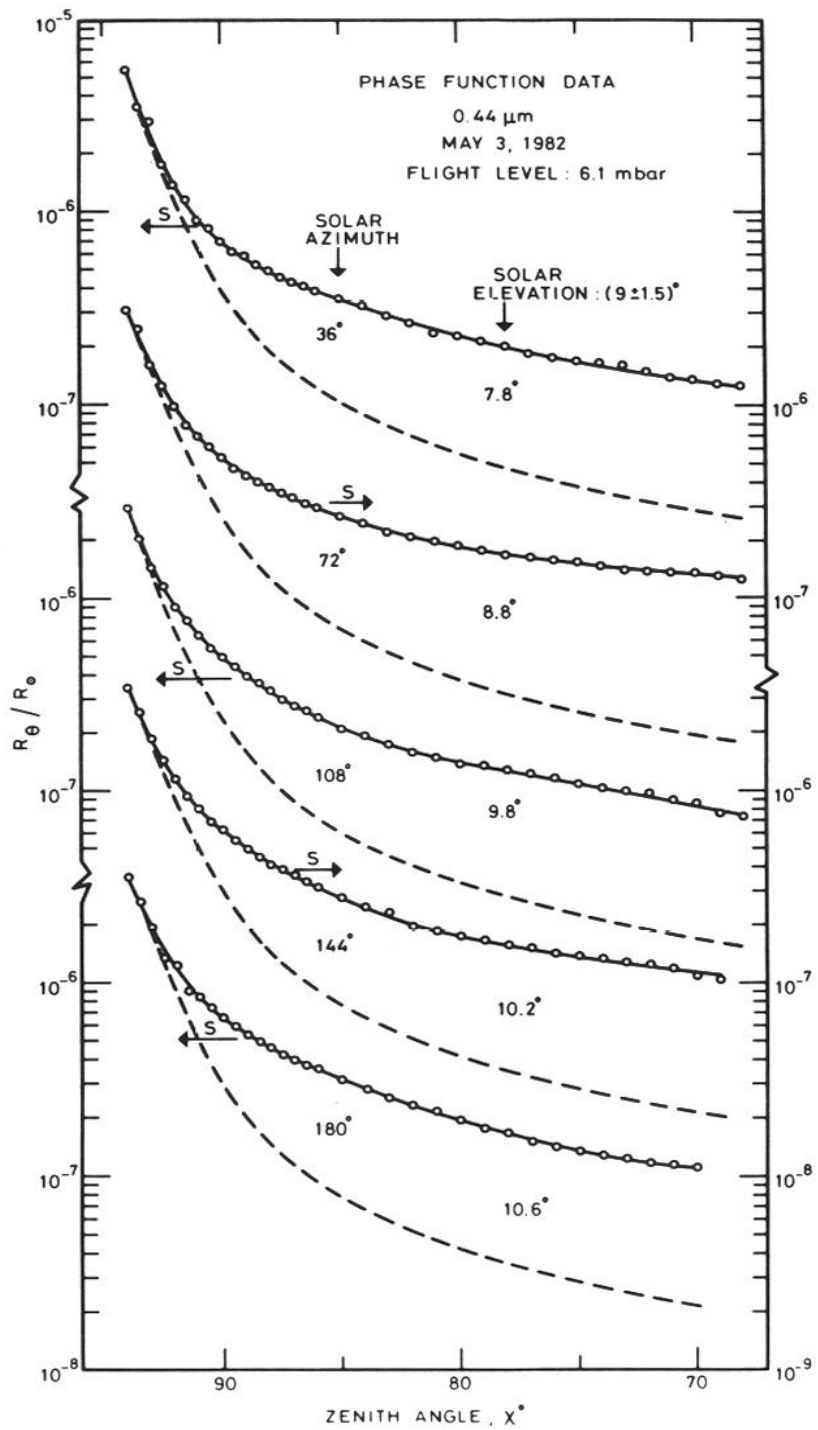


FIG. 12. — As in figure 8 the 0.44 μm observed radiance is shown versus zenith angles. In this case the data obtained at various solar azimuth angles are shown which will serve as a basis for the phase function determination of the excess radiance.

the phase function at zenith angles close to 93.5° corresponding to grazing altitudes nearing 20 km at these low altitudes the earth sphericity induces illumination asymmetries when the solar azimuth changes from 36° to 180° . This most probably explains the deformation of the air phase function shown in figure 13 for air. At smaller zenith angles the air Rayleigh scattering becomes quickly very small compared with the excess radiance for which it becomes only a correction factor. The phase function observed at $\chi = 80^\circ$ is for this reason used to deduce its characteristics.

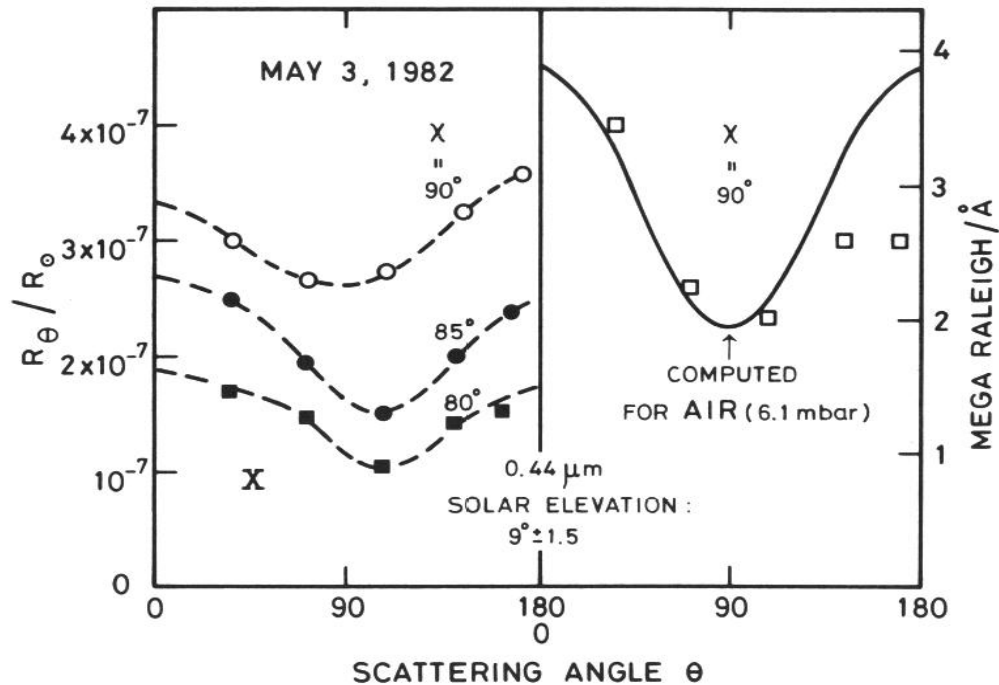


FIG. 13. — Atmospheric excess radiance (X) observed at various zenith angles versus scattering angles θ° . The pure air radiance phase function computed for the flight level from the air differential cross section (25) is also shown with the observation (see text).

The value of $Q_s n \sigma$ has been evaluated from these experimental data by means of the relationship.

$$Q_s n \sigma = 1.85 \times 10^5 \sum_0^{180} (R_\theta / R_\odot) (\sin \theta \sin \Delta\theta / 2) \quad (6)$$

by zonal summation every 10° from 0° to 180° . The extinction due to scattering is found to be 2.6×10^{-2} which, according to figure 10, leads to $Q_s n \sigma$ at $\chi = 90^\circ$ equal to 6.1×10^{-2} . On the other hand, the asymmetry parameter, $\langle \cos \alpha \rangle$, is found to be equal to 0.06.

4. DISCUSSION OF THE DATA

The extinction and the excess of radiance have been shown to originate from an altitude near 60 km, in the mesosphere. They both have also in common to exhibit a large enhancement when the wavelength changes from 0.65 μm to 0.44 μm .

For an effective height of 60 km and an observation altitude of 35 km the optical depth factor increases 11.4 times from $\chi = 0^\circ$ to $\chi = 90^\circ$. The excess extinction observed leads, according to figure 4 to a zenithal optical depth equal to 6.6×10^{-2} of which 5.4×10^{-3} is due to scattering by the dust layer. If it is accepted that the dust is responsible for both extinction and scattering in the 60 km layer, the dust scattering albedo is equal to 0.08. This low value is compatible with very small particles exhibiting an almost symmetric scattering phase function. One way to explain the large scattering efficiency increase when the wavelength changes from 0.65 to 0.44 μm is to consider a colour dependent complex index of refraction in this range with a non negligible imaginary part of the index [26]. The dust would thus be made out of brownish matter. The complexity of upper atmospheric dust most probably from extraterrestrial origin has already been pointed out [27].

CONCLUSION

The demonstration of the presence in the earth atmosphere of a dust layer at 60 km altitude would have a purely academic interest. Its association with a non negligible sunlight extinction and absorption in situ makes it important for the earth radiation balance, for the stratospheric and mesospheric photochemistry and energy budget and for the measurements of stratospheric trace species in blue light.

These aspects justify fully to continue the optical investigation of the layer from balloon gondola and from other platforms and to use other methods of investigation.

ACKNOWLEDGEMENTS

We thank the french Centre National d'Études Spatiales for the balloon operations and the Établissement d'Études et de Recherches Météorologiques for atmospheric soundings.

REFERENCES

- [1] VOLZ, F. and GOODY, R. M., 1962. *J. Atmos. Sci.*, **19**, 385-406.
- [2] GIOVANE, F., SCHUERMAN, D. W. and GREENBERG, J. M., 1976. *J. Geophys. Res.*, **81**, 5383-5388.
- [3] KONDRATYEV, J. Ja, BUZNIKOV, A. A. and POKROVSKY, O. M., 1977. *Doklady A.N.S.S.S.R.*, **235**, 53-56.
- [4] GRAY, C. R., MALCHOW, H. L., MERRITT, D. C. and VAR, R. E., 1973. *Spacecraft and Rockets*, **10**, nr 1.
- [5] CUNNOLD, D. M., GRAY, C. R. and MERRITT, D. C., 1973. *Geophys. Res.*, **78**, 920-931.
- [6] ROSSLER, F., 1967. *The Aerosol-Layer in the Stratosphere*, Deutsch-Französisches Forschungsinstitut, St Louis, France.
- [7] MEINEL, M. P. and MEINEL, A. B., 1963. *Science*, **142**, 582-583.
- [8] HUNTEN, D. M., TURCO, R. P. and TOON, O. B., 1980. *J. Atm. Sci.*, **37**, 1342-1357.
- [9] VASSY, A. and E., 1939. *Journal de Physique*, **10**, 403-412.
- [10] DUNKELMAN, L. and SCOLNIK, R. J., 1959. *Opt. Soc. Am.*, **49**, 356-367.
- [11] LABS, D. and NECKEL, H., 1968. *Z. Astrophysik*, **69**, 1-73.
- [12] DELUISE, J. J., 1975. *J. Geophys. Res.*, **80**, 345-354.
- [13] BLAMONT, J., POMMERAU, J. P. and SOUCHON, G., 1975. *C.R. Acad. Sc.*, Paris, **281**, 247-252.
- [14] LEROY, B., HICKS, E. and VASSY, A., 1980. *Ann. Geophys.*, **36**, 205-208.
- [15] ACKERMAN, M. and MULLER, C., 1972. *Nature*, **240**, 300.
- [16] ACKERMAN, M., FONTANELLA, J. C., FRIMOUT, D., GIRARD, A., LOUISNARD, N. and MULLER, C., 1975. *Planet. Space Sci.*, **23**, 651-660.
- [17] COFFEY, M. T., MANKIN, W. G. and GOLDMAN, A., 1981. *J. Geophys. Res.*, **86**, 7331-7341.
- [18] NOXON, J. F., 1975. *Science*, **189**, 547-549.
- [19] KERR, J. B. and McELROY, C. T., 1976. *Atmosphere*, **14**, 166-171.
- [20] GOLDMAN, A., FERNALD, F. G., WILLIAMS, W. J. and MURCRAY, D. G., 1978. *Geophys. Res. Lett.*, **5**, 257-260.
- [21] RIGAUD, P., NAUDET, J. P. and HUGENIN, D., 1977. *C.R. Acad. Sc. Paris*, **284**, 331-334.
- [22] NAUDET, J. P., RIGAUD, P. and HUGENIN, D., 1978. *Geophys. Res. Lett.*, **7**, 701-703.
- [23] POMMERAU, J. P., 1981. *Thesis*, University of Paris VI.
- [24] ACKERMAN, M., LIPPENS, C. and MULLER, C., 1981. *Nature*, **292**, 587-591.
- [25] PENNDORF, R., 1957. *J. Opt. Soc. Ann.*, **47**, 176-183.
- [26] KERKER, M., 1969. *The scattering of light and other electromagnetic radiation*, Academic Press, New York-London.
- [27] BIGG, E. K., KVIZ, Z. and THOMPSON, W. J., 1971. *Tellus*, **23**, 247-259.